5-1-2007

Doubly Differential Single and Multiple Ionization of Krypton by Electron Impact

O. G. de Lucio

Jared M. Gavin

Robert D. DuBois
Missouri University of Science and Technology, dubois@mst.edu

Doubly differential single and multiple ionization of krypton by electron impact

O. G. de Lucio, J. Gavin, and R. D. DuBois
University of Missouri-Rolla, Rolla, Missouri 65409, USA
(Received 7 March 2007; published 15 May 2007)

Differential measurements for single and multiple ionization of Kr by 240 and 500 eV electron impact are presented. Using a pulsed extraction field, Kr^+, Kr^{2+}, and Kr^{3+} ions were measured in coincidence with scattered electrons for energy losses up to 120 eV and scattering angles between 16° and 90°. Scaling properties of the doubly differential cross sections (DDCS) are investigated as a function of energy loss, scattering angle, and momentum transfer. It is shown that scaling the DDCS as outlined by Kim and Inokuti and plotting them versus a parameter consisting of the momentum transfer divided by the square root of the impact energy times $1-\cos(\theta)$, where θ is the scattering angle, yielded similar curves, but with different magnitudes, for single and multiple ionization. Normalizing these curves together produced two universal curves, one appropriate for single and multiple electron emission at larger scattering angles ($\theta \geqslant 30°$) and one appropriate for small scattering angles ($\theta < 30°$).

DOI: 10.1103/PhysRevA.75.052709 PACS number(s): 34.80.Dp

I. INTRODUCTION

Ionization of atoms and molecules is one of the basic processes in atomic physics. Thus it has been extensively studied, both experimentally and theoretically, for nearly 100 yrs. From the view point of applied science, how atoms and molecules respond to collisional energy deposition is of interest in several fields of physics and chemistry, such as astrophysics, atmospheric science, radiation effects on matter, plasma and chemical processes. From an academic point of view, the study of the dynamics of the electron-atom inelastic scattering lead to a better understanding of the physical structure of atoms and molecules and how energy and momentum are transferred between atomic particles during a collision. In both cases, differential information about the energy deposition and response are required.

Experimentally, by measuring the electron emission as a function of emission energy and angle, electron and ion impact ionization studies have provided such information for many systems and impact energies. Electron-electron coincidence experiments, usually known as $(e,2e)$ experiments, have proven to be one of the most powerful tools for these studies [1] since they separate out various ionization channels and correlate the physical properties of the particles before and after the interaction. The pioneering experiments of Ehrhardt [2] initiated these experimental efforts and numerous theoretical approaches have been used [3–8]. Often, the theories are based on perturbation models such as the Born, binary encounter, and other models. The reader is referred to the reviews of Weng *et al.* [9], Kim and Inokuti [10], and Inokuti *et al.* [11,12] for specific details of the various models and about how the cross sections scale as a function of target species, energy deposition, etc. In general, the models provide scaling properties about the amount of energy deposited due to single ionization of a particular shell. Therefore they are most appropriate for light atoms. For heavier atoms contributions from the various shells can be calculated and summed, but with the restriction that only single ionization processes occur. Multiple ionization processes are much more difficult to model since they can be achieved from various processes such as direct multiple ionization [13,14] which may, or may not, involve correlation between electrons [15], ionization of inner shells followed by Coster-Kronig [16] or Auger [17] transitions, resonant excitation [18], and shake off ionization [19]. Thus, although calculations for specific systems and conditions can sometimes be made, generalized scaling properties for angular distributions and particularly for multiple ionization processes are generally not provided by these models. Thus, an adequate description of the multiple ionization process for targets heavier than H and He represents a major challenge The purpose of this work is to provide insight into developing these theoretical capabilities by providing highly differential information about single and multiple ionization of a heavy atom, Kr, resulting from electron impact.

For krypton, a considerable number of previous measurements for total cross sections of single and multiple ionization induced by electron impact can be found on the literature. Syage [20] reported cross sections as a function of the impact energy from threshold to 470 eV for single and multiple (2+ to 6+) ionization of Kr and Xe; Tinschert, *et al.* [21] measured single ionization of different Kr ions ($q=1-3+$) in the energy range from threshold to 700 eV; and Krishnakumar and Srivastava [22] reported total cross sections for selected rare gas atoms resulting from electron impact energies ranging from threshold to 1000 eV. They also presented a compilation of earlier measurements.

In contrast there are only a few published results in the literature involving differential experimental data for single and multiple ionization of Kr atoms by electron impact. For example El-Sherbini and Van der Wiel [23] have reported measurements for small angle, inelastic scattering of 10 keV electrons colliding with Kr and Xe targets. They determined oscillator strengths for charge states 1+ to 4+. In a different study Chaudry *et al.* [24] published measurements of partial doubly differential cross sections for ionization of Ar, Kr, and Xe. They employed projectiles with energies ranging from 0.5 keV to 10 keV and the ejected electrons were detected at a fixed angle of 90° with respect to the beam direction. Their resultant cross sections are normalized and pre-

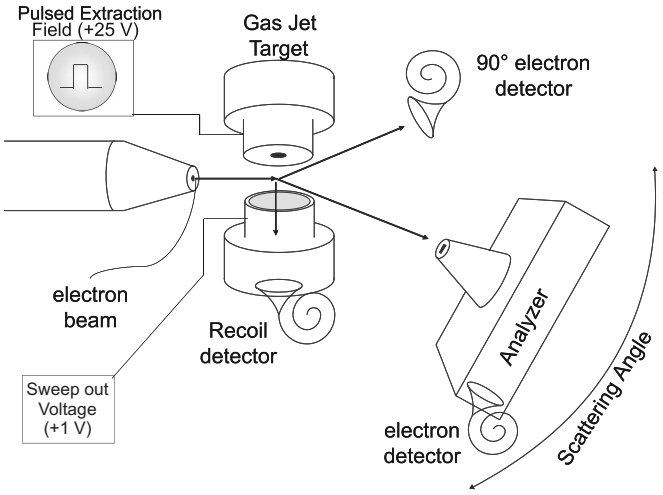

FIG. 1. Diagram of the experimental apparatus.

sented as a function of the ejected electron energy. More recently our group has reported measurements of doubly differential single and multiple ionization cross sections for 750 eV electron and positron impact on Kr atoms [25] as a function of energy loss and scattering angle.

Although these previous differential studies provide valuable information, they generally have probed only a single or a limited set of parameters, such as a single electron emission angle or energy or a single impact energy. The purpose of the present work is to supplement the available information about differential ionization of heavy atoms and to investigate whether scaling properties of these data can be established. This is important since it is impractical to measure every possible combination of projectile and ejected electron energies, emission angles and ionization states. Determining various scaling properties in order to generate a "*universal curve*" for differential electron emission for multiple, as well as single, ionization of heavier atoms is the ultimate goal of the present work.

For this purpose, we have measured doubly differential cross sections (DDCS) for both single and multiple ionization of Kr resulting from 240 and 500 eV electron impact. To investigate scaling properties, results for various energy losses ranging from near threshold up to about 120 eV and for scattering angles between 16.5° and 90° degrees with respect to the beam direction are studied as a function of momentum transfer, as a function of energy loss and as a function of scattering angle. In addition, we present the experimental results as a function of a variable which includes both the momentum transfer and scattering angle.

II. EXPERIMENTAL PROCEDURE AND DETAILS

The experimental apparatus is shown schematically in Fig. 1. An electron beam, typically about 2×10^{-12} A and 0.5 mm in diameter, was passed through the interaction region which consisted of two coaxial cylinders separated by a distance of 6 mm. The Kr target consisted of a simple gas jet which was injected into the interaction region through a 1 mm aperture in the top cylinder. Ionized atoms were extracted through a 5 mm aperture in the bottom cylinder and then detected using a channel electron multiplier. The front of this recoil ion detector was biased at −2.2 kV and was located at about 6 mm from the extraction region to achieve time focusing of the extracted ions. Detection efficiencies for singly and multiply charged krypton ions were taken from [26].

After passing through the interaction region, scattered electrons were energy analyzed and detected using a parallel-plate spectrometer and a channel electron multiplier. The spectrometer could be positioned at angles ranging from 0° to 90° measured with respect to the beam direction. The energy acceptance was ±6% of the energy of the scattered electron and the angular resolution was ±2°.

Upon detection of a scattered electron, an extraction pulse of magnitude +25 V and width of 15 μsec was applied to the top cylinder of the extraction region; this pushes any Kr ions in the interaction region towards the recoil ion detector. Using the scattered electron signal as a start and the recoil ion signal as a stop to trigger a time to amplitude converter (TAC), recoil time-of-flight (TOF) spectra were acquired. By measuring spectra using extraction pulse widths from 5 to 60 μsec, it was found that for widths shorter than 10 μsec a noticeable decrease of the coincidence rate per pulse width occurred while for widths larger than 20 μsec a "tail" corresponding to longer flight times appeared next to the single ionization peak. The above pulse amplitude and width were found to be adequate for extracting the slowest ion of interest, Kr^+. Capacitance pickup of the extraction pulse by the electron and ion detectors was avoided by adding extra shielding to the cables carrying the pulse voltage and those connected to the various detectors, plus by a shielding enclosure surrounding the recoil ion detector. Typically, the induced background signals measured at the output of the recoil ion detector had amplitudes less than 10 mV for a 60 V ion extraction pulse. The electron detector was further away and better shielded, thus the induced signals were smaller.

To remove any ions remaining in the interaction region which were produced in earlier interactions or by electrons not detected, a dc "sweep out" voltage of +1 V was applied to the bottom cylinder. For selecting this voltage it needed to be large enough to remove these residual ions but small enough so the main beam was not deflected. Voltages between +0.4 V and +1.5 V were shown to provide identical results; using negative voltages resulted in a high intensity background in the spectra; high positive voltages (>+5 V) produced completely deformed spectra where the peaks that could not be associated with any particular ionization state. Plus, the importance of using a sweep out voltage was evident when spectra acquired without it showed the production of Kr^{2+} and Kr^{3+} ions, even when the energy loss was below the threshold to produce such states.

The procedure used was the following. The beam energy was set, the target was stabilized at a fixed pressure, the electron spectrometer was rotated to a fixed angle, θ, and the spectrometer voltage was adjusted to measure a particular energy loss, ε. Then, the beam intensity was adjusted such that the recoil ion rate for a dc extraction field was around 15 000 counts/second. The recoil ion extraction pulse volt-

age was turned on and scattered electrons and recoil ions were measured in coincidence thus generating TOF spectrum for each combination of projectile energy, energy loss and scattering angle of interest were collected. Peaks in the spectra were associated with various ionization charge states, q. For the Kr^{3+} it was necessary to subtract contributions due to N_2^+, which is present as a background gas in the vacuum system, in order to do so the procedure outlined in [25] was followed.

The background subtracted TOF peak intensities, $N_{\varepsilon\theta q}$, divided by the respective recoil ion detection efficiencies, η_q, is proportional to the number of ejected electrons for each degree of ionization; their sum being proportional to the probability of a single or multiple ionization event where one of the electrons has suffered a particular energy loss and is scattered into a particular angle. Charge state fractions as a function of energy loss and scattering angle, $f_{\varepsilon\theta q}$, were then obtained by dividing these values by their sum, $\Sigma_q \frac{N_{\varepsilon\theta q}}{\eta_q}$, which is equal to the number of electrons detected at angle θ, $N_{\varepsilon\theta}$. The integrated TOF peak intensities were converted to absolute cross sections using a normalization procedure employing noncoincidence measurements and known total ionization cross sections.

The first step of the normalization process was to measure the ratio of the number of electrons detected for each scattering angle and energy loss combination, $N_{\varepsilon\theta}$, to the number of electrons detected by a channel electron multiplier positioned at 90° with respect to the beam, but on the opposite side of the beam axis from the rotatable detector. In order to limit the electron signal, the front of the 90° detector was biased at a negative voltage of about 60% of the beam energy, thus allowing electrons for a range of energies to be counted, $N_{\Sigma\varepsilon 90}$. We define the ratio $N_{\varepsilon\theta}/N_{\Sigma\varepsilon 90}$ as $R_{\varepsilon\theta 90}$. Note that dividing by the 90° electron signal normalizes all the coincidence data to a constant value for the overlap intensity of the electron beam and target jet. To place the data on an absolute scale, the ratio of the 90° electron yield divided by the recoil ion yield, N_I, i.e., R_{90ion}, was measured. Since N_I is proportional to known partial ionization cross sections, this normalization placed all the differential data on an absolute scale.

$N_{\varepsilon\theta q}$ is related to the differential electron emission cross section for a particular emission energy, emission angle and degree of ionization, $\frac{d^2\sigma_q}{d\varepsilon d\Omega}$, while N_I is related to the total cross sections for single and multiple ionization, σ_q, in the following manner

$$N_{\varepsilon\theta q} = \frac{d^2\sigma_q}{d\varepsilon d\Omega} N_B N_T q \Delta\varepsilon \Delta\Omega \eta_e 4\pi \eta_q, \tag{1}$$

$$N_I = \sum_q N_q = \sum_q \sigma N_B N_T 4\pi \eta_q. \tag{2}$$

Here N_B and N_T are the number of beam and target gas particles; $\Delta\varepsilon$ and $\Delta\Omega$ are the energy acceptance and solid angle for which data are collected; η_e and η_q are the detection efficiencies, including any transmission effects, for electrons and recoil ions. Finally, 4π is the solid angle for detecting recoil ions and the q included in Eq. (1) accounts for multiple ionization events where q electrons are liberated. Dividing Eq. (1) by $\Sigma_q \frac{N_{\varepsilon\theta q}}{\eta_q}$ and then by Eq. (2) and rearranging yields

$$\frac{d^2\sigma_q}{d\varepsilon d\Omega} = \frac{f_{\varepsilon\theta q} R_{\varepsilon\theta 90} R_{90\ \mathrm{ion}}}{q \eta_q \Delta\varepsilon \Delta\Omega \eta_e} \sum_q \sigma_q \eta_q. \tag{3}$$

The detector efficiencies, η_e and η_q, were obtained from [26,27], electron detection efficiencies were found to be rather constant between 100 eV and several hundred eV. Variations were less than statistical uncertainties in our data so were not taken into account. With regard to detection efficiencies for different detectors we are not aware of any direct comparisons but various literature values do not imply that differences for detecting electrons are expected. The partial cross sections σ_q were taken from the work of Rejoub *et al.* [28] with all other quantities being measured during the present work.

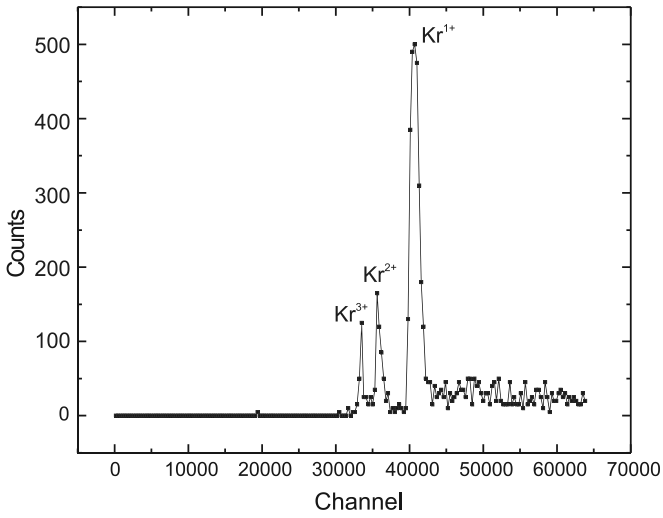

FIG. 2. Kr TOF spectrum for 500 eV electron beam. The corresponding energy loss for this spectrum is 77 eV and the scattering angle is 16.5°.

III. RESULTS

A typical TOF spectrum is shown in Fig. 2. Although not shown, the general trends of $f_{\varepsilon\theta q}$ as a function of energy loss that was observed for all scattering angles are: (a) the single ionization fraction decreases slowly and becomes practically constant for high energy losses, (b) initially the double ionization fraction increases rapidly and then within uncertainties also becomes constant for high energy losses, (c) in its threshold region the triple ionization fraction does not appear to increase as fast double ionization does and for high energy losses it is difficult to tell if it also reaches a constant value due to lack of sufficient data.

Using this procedure, single, double and triple ionization cross sections of Kr by 240 and 500 eV were determined as a function of scattering angle and energy loss. Figures 3 and 4 show the DDCS plotted in the traditional manner, e.g., as a function of the energy loss and as a function of the scattering

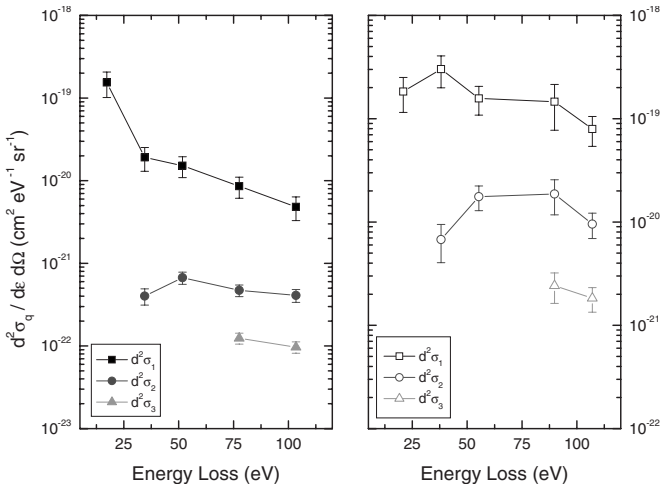

FIG. 3. Doubly differential cross sections of the different ionization states of Kr as a function of the energy loss for 500 eV (left) and 240 eV (right) electron impact. All the data corresponds to a 33° scattering angle.

angle. The lines in the figures simply connect the data points. Here can be noticed the differences on the DDCS for different combinations of bombardment energies, energy loss and momentum transfer, as well as the relative ratios for different ionization states. With regard to double and triple ionization, any influence on the present experimental data by inner shell processes such as the Auger emission can be ruled out because known Auger transitions energies, e.g., M_1-N_1N_1 (27.1 eV), M_2-$N_{23}N_{23}$ (54.9 eV), M_3-$N_{23}N_{23}$ (62.7 eV), M_2-N_1N_{23} (71.1 eV), M_1-$M_{45}N_{23}$ (74.8 eV) and M_3-N_1N_{23} (78.9 eV) [29], do not coincide with the energy loss regions we investigated.

As seen, when plotted as a function of energy loss the data demonstrate different features for different impact energies and degrees of ionization. With respect to the angular

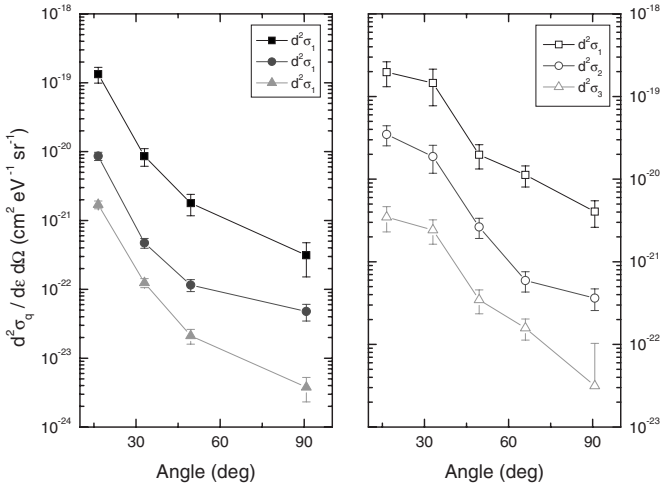

FIG. 4. Doubly differential cross sections of the different ionization states of Kr as a function of the scattering angle for 500 eV (left) and 240 eV (right) electron impact. The left side corresponds to an energy loss of 77 eV and the data on the right to an energy loss of 89 eV.

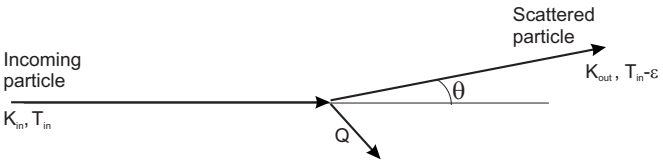

FIG. 5. Quantities involved in the collision process (not to scale). The incoming particle has an initial momentum K_{in} and initial energy T_{in}. After the collision the projectile is scattered by an angle θ, and will have a final momentum K_{out} and energy $T_{in}-\varepsilon$, where ε is the energy loss during the collision. Finally, the momentum transfer is represented by Q.

dependence, the DDCS' exhibit a monotonically decrease with respect to the scattering angle. Comparing the 500 and 240 eV data, the main difference is at low scattering angles. Thus, the DDCS do not scale as simple functions of scattering angle or energy loss. Although not shown, the data were also plotted as a function of momentum transfer, Q; but again no simple scaling function was apparent.

In order to construct a more universal representation, a procedure as outlined by Kim and Inokuti [30] was used. First, the DDCS were multiplied by the following coefficient:

$$Z(T_{\rm in},\varepsilon) = T_{\rm in}\left(\frac{(T_{\rm in}-\varepsilon)^2}{4\pi a_0^2 {\rm Ry}^2}\right), \tag{4}$$

where T_{in} is the beam energy, ε the projectile energy loss, a_0 the Bohr radius and Ry the Rydberg energy. For the same degree of ionization, this shifts the data for different impact energies to the same vertical level. But the curves for different scattering angles are still shifted horizontally with respect to each other. It was found that the horizontal shift could be accounted for by introducing a "reduced momentum transfer," $Q_{\rm red}$, defined by

$$Q_{\rm red} = \frac{Q}{T_{\rm in}^{1/2}(1-\cos\theta)^{1/2}}. \tag{5}$$

Here the momentum transfer Q, defined as $Q=K_{in}-K_{out}$ (see Fig. 5) is in atomic units, T_{in} is the incoming energy of the projectile, and θ is the scattering angle.

Plotting $Z(T_{\rm in},\varepsilon)\frac{d^2\sigma_q}{d\varepsilon d\Omega}$ as a function of $Q_{\rm red}$ compressed the data for all energy losses and scattering angles into three similarly shaped curves, one for single ionization, one for double ionization, and one for triple ionization. Finally, at each bombardment energy, the double and triple ionization curves were normalized to the single ionization curve with the results shown in Figs. 6 and 7. In both cases, the individual measurements were binned and averaged where possible with the average values being plotted. Observe that scaling the cross sections in this manner and plotting them versus this new variable compresses all the DDCS for different combinations of energy loss, scattering angle and bombardment energy into two curves. One curve, where $Q_{\rm red} < 1.4$, is monotonically increasing and is depicted in Fig. 6. This curve corresponds to large scattering angles (>30°). The other curve is monotonically decreasing as shown in Fig. 7. This curve is for small scattering angles (<30°) and

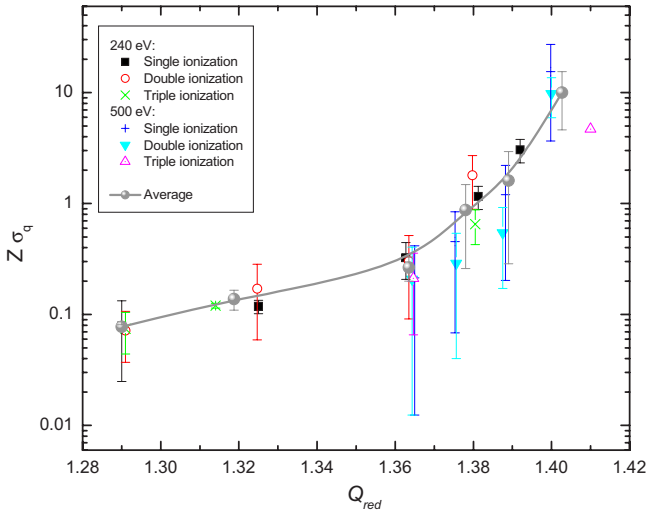

FIG. 6. (Color online) Normalized DDCS plotted as a function of the Q_{red} variable for scattering angles $\theta \geqslant 30°$. The dots connected by a solid line represent the average of the different normalized curves.

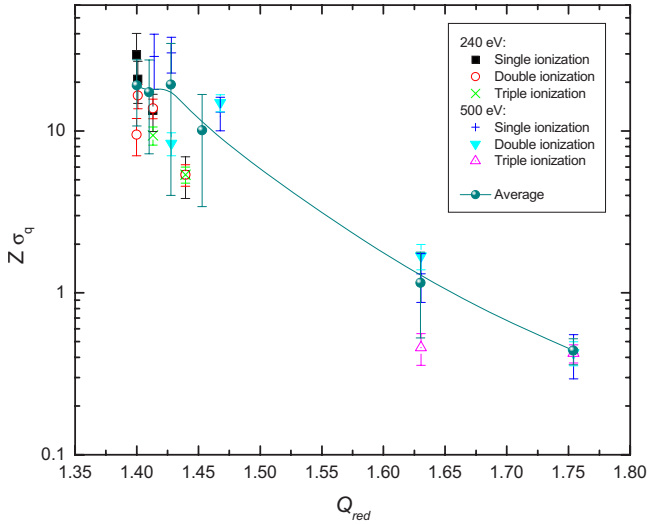

FIG. 7. (Color online) Normalized DDCS plotted as a function of the Q_{red} variable for scattering angles $\theta < 30°$. The dots connected by a solid line represent the average of the different normalized curves.

for values of $Q_{\mathrm{red}} > 1.4$. Although not included here, we tested this scaling further by using 250 and 500 eV electron impact data for ionization of Ar. Similar results were obtained. We should comment that the denominator used to calculate Q_{red} is similar to the parallel component of the momentum transfer, but our attempts to find a better scaling function using Q/Q_{parallel} were unsuccessful.

IV. SUMMARY AND CONCLUSIONS

New data for differential single and multiple ionization of Kr as a function of energy loss and scattering angle have been presented. The data are for 240 and 500 eV electron impact. Plots of these data as functions of energy loss, scattering angle, and momentum transfer demonstrated some similarities but also many differences. However, it was shown that by scaling the cross sections according the procedures outlined by Kim and Inokuti and plotting them versus a reduced momentum transfer, similarly shaped curves for single, double, and triple ionization resulted. After these curves were normalized together (in magnitude), two "universal" curves were found. One curve which is monotonically increasing, corresponded to large, $>30°$, scattering angles, the other which is monotonically decreasing, to small, $<30°$, scattering angles. As a result, DDCS for single and multiple ionization of a heavy atom could be compressed by several orders of magnitude to produce two universal curves. The present results were obtained for energy losses up to approximately a third of the initial energy, scattering angles between 16° and 90°, and two impact energies. Further studies are required to establish the overall applicability of this method with respect to the range of energy losses, scattering angles, impact energies, and targets. However, to our knowledge this is the first demonstration of a scaling method which is applicable to differential electron emission resulting from multiple, as well as single, ionization of a heavy atom. It is hoped that the procedures outlined here will aid in theoretical methods for calculating single and multiple inelastic electron processes occurring in heavy atoms.

[1] C. T. Whelan, R. J. Allan, H. R. J. Walters, and X. Zhang, (*e*,2*e*) *and Related Processes*, edited by C. T. Whelan, H. R. J. Walters, A. Lahmam-Bennani, and H. Ehrhardt (Kluwer Academic, Dordrecht, 1993).
[2] H. Erhardt, M. Schulz, T. Tekaat, and K. Willmann, Phys. Rev. Lett. **22**, 89 (1969).
[3] N. R. Badnell, D. C. Griffin, and M. S. Pindzola, J. Phys. B **24**, 275 (1991).
[4] P. Defrance, W. Claeys, A. Cornet, and G. Poulaert, J. Phys. B **14**, 111 (1981).
[5] S. M. Younger, Phys. Rev. A **22**, 111 (1980).
[6] S. M. Younger, Phys. Rev. A **22**, 1425 (1980).
[7] J. Botero and J. H. Macek, Phys. Rev. Lett. **68**, 576 (1992).
[8] W. Hu, D. Fang., Y. Wang, and F. Yang, Phys. Rev. A **49**, 989 (1994).
[9] M. S. Weng, A. Schinner, A. Sharma, and P. Sigmund, Eur. Phys. J. D **39**, 209 (2006).
[10] Y. K. Kim and M. Inokuti, Phys. Rev. A **3**, 665 (1971).
[11] M. Inokuti, Rev. Mod. Phys. **43**, 297 (1971).
[12] M. Inokuti, Y. Itikawa, and J. E. Turner, Rev. Mod. Phys. **50**, 23 (1978).
[13] F. D. Daniel, Nucl. Instrum. Methods Phys. Res. **214**, 57 (1983).
[14] A. Kumar and B. N. Roy, Can. J. Phys. **56**, 1255 (1978).
[15] V. Schmidt, N. Sandner, H. Kuntzemüller, P. Dhez, F. Wiuelleuumier, and E. Kallne, Phys. Rev. A **13**, 1748 (1976).

[16] W. Melhorn, Z. Phys. **208**, 1 (1967).
[17] W. Melhorn in *Lectures on the Auger Effect* (University of Nebraska, Lincoln, 1969).
[18] S. S. Tayal and R. J. W. Henry, Phys. Rev. A **44**, 2955 (1991).
[19] T. A. Carlson and C. W. Nester, Phys. Rev. A **8**, 2887 (1973).
[20] J. A. Syage, Phys. Rev. A **46**, 5666 (1992).
[21] K. Tinschert, A. Müller, G. Hoffmann, Ch. Achenbach, R. Becker, and E. Salzborn, J. Phys. B **20**, 1121 (1987).
[22] E. Krishnakumar and S. K. Srivastava, J. Phys. B **21**, 1055 (1988), and references therein.
[23] Th. M. El-Sherbini and M. J. Van der Wiel, Physica (Amsterdam) **62**, 119 (1972).
[24] M. A. Chaudhry, A. J. Duncan, R. Hippler, and H. Kleinpoppen, Phys. Rev. A **39**, 530 (1989).
[25] A. C. F. Santos, A. Hasan, and R. D. DuBois, Phys. Rev. A **69**, 032706 (2004).
[26] M. Krems, J. Zirbel, M. Thomason, and R. D. DuBois, Rev. Sci. Instrum. **76**, 093305 (2005).
[27] R. D. DuBois, Ph.D. thesis, University of Nebraska, 1975.
[28] R. Rejoub, B. G. Lindsay, and R. F. Stebbings, Phys. Rev. A **65**, 042713 (2002).
[29] F. P. Larkins, J. Phys. B **6**, 1556 (1973).
[30] Y. K. Kim and M. Inokuti, Phys. Rev. A **7**, 1257 (1973).